American Mineralogist, Volume 81, pages 632–638, 1996

Structure refinement of a natural K-rich diopside: The effect of K on the average structure

GEORGE E. HARLOW

Department of Earth and Planetary Sciences, American Museum of Natural History, New York, New York 10024-5192, U.S.A.

ABSTRACT

The crystal structure of the most K-rich natural pyroxene ever reported, a chromian diopside with 1.5 wt% K_2O, has been refined (diffractometer data, filtered Mo$K\alpha$ radiation, by least-squares using XTAL to R_u = 3.2%) to examine the effect of K on the average structure. The crystal with structural formula $Ca_{0.80}K_{0.073}Na_{0.023}Mg_{0.95}Fe_{0.06}Cr_{0.07}Al_{0.02}Si_2O_6$ was found as an inclusion in a Koffiefontein diamond. The refined structure is typical of clinopyroxene on the diopside-enstatite join: Mg in M2 leads to distortion that is modeled by site splitting, with M2′ (Mg + Fe) displaced 0.33 Å from M2 (Ca + K + Na). Assignment of K to M2 is required to account for the electron density at that site. The average of eight M2-O distances (2.504 Å) is slightly larger than for diopside (2.498 Å). The effect of K on the average M2-O distance can be seen by calculating the average cation radius of atoms at M2 (+ M2′) from the occupancy: 0.798·1.12 Å ($^{[8]}$Ca) + 0.073·1.51 (K) + 0.023·1.18 (Na) + 0.036·0.92 (Fe) + 0.070·0.89 (Mg) = 1.127 $\sim\geq R$ ($^{[8]}$Ca). The large size of K is mostly offset by Mg + Fe in M2′ in the diopside-like structure; this size-distortion balancing may facilitate K uptake in mantle clinopyroxene in K-rich environments. Large apparent thermal motion parameters of most atomic sites indicate sizable local distortions of the structure from substitution of K into M2.

INTRODUCTION

Clinopyroxene (Cpx) has not been considered a major crystal-chemical reservoir for K because the preponderance of compositional data for pyroxenes of all kinds has shown only trace K content. The crystal-chemical reasoning is that K^+ (radius $^{[8]}K^+$ = 1.51 Å; Shannon 1976) is too large to enter the largest site, M2, in the pyroxene structure. Recently, Harlow and Veblen (1991) showed that K^+ at levels of at least 0.08 cations per six O atoms can reside in the crystal structure of clinopyroxene included in diamond and, thus, have confirmed the accuracy of some analyses of mantle clinopyroxene with substantial K_2O (e.g., Prinz et al. 1975; McCandless and Gurney 1986; Rickard et al. 1989; Sobolev et al. 1991). Harlow and Veblen (1991) reasoned that high pressure and a K-rich environment were required to yield the K-rich pyroxenes found in diamonds. In addition, they proposed that K uptake should be favored in a more expanded pyroxene structure, which is correlated with a large cell volume, such as that of diopside, and a relatively large charge-balancing M1 cation, such as Cr^{3+}. In the present study the crystal structure of the most K-rich natural pyroxene recorded (Rickard et al. 1989) has been refined from three-dimensional single-crystal X-ray diffraction data to confirm that K indeed enters the structure and to examine the effects of the large K^+ ion on the structure.

DESCRIPTION

The single diopside crystal K18a used in this study was extracted from a diamond from the Koffiefontein pipe in South Africa and was described and analyzed by Harlow and Veblen (1991) and Rickard et al. (1989). Originally, K18a was a relatively large crystal, 250 μm maximum dimension, containing a lath of orthopyroxene (Opx); however, owing to strain it spontaneously "popped" while mounted on the diffractometer, losing most of its mass and the Opx lamella. In its final form it was an irregular gemmy green crystal (see Table 1). The microprobe compositions of the Cpx crystal are very uniform (see Harlow and Veblen 1991) and yield a structural formula of $Ca_{0.80}K_{0.073}Na_{0.023}Mg_{0.95}Fe_{0.06}Cr_{0.07}Al_{0.02}Si_{1.99}O_6$.

X-RAY AND REFINEMENT METHODS

The crystal was examined by single-crystal X-ray diffraction to evaluate both crystallinity and lattice dimensions before intensity measurements. Long-exposure (>100 h) precession photographs (Mo$K\alpha$, Zr filter) showed only sharp Bragg diffraction intensities consistent with space group $C2/c$. Lattice dimensions were refined using LCLSQ from 31 diffractions [0.69 > (sin θ)/λ > 0.43] measured on the diffractometer (average of $\pm 2\theta$) and are listed in Table 1.

X-ray intensity data from a hemisphere of reciprocal space were measured on a Krisel-automated Picker

0003–004X/96/0506–0632$02.00

TABLE 1. Experimental details for K18a diopside

Space group	*C*2/*c*
Lattice dimensions:	
a (Å)	9.7476(4)
b (Å)	8.9478(4)
c (Å)	5.2622(2)
β (°)	106.056(2)
V (Å^3)	441.06(3)
Radiation	Mo$K\alpha$ (Zr filter) 2000 Watts
Crystal dimensions	150 × 130 × 80 μm
2θ range	5-65°
Scan type	θ-2θ
Scan width 2θ (°)	2.0° + 0.70(tan θ)
Scan duration	≤180 s
Intensity standards	3 per 5 h
Total reflections	1538
Unique reflections	667
R_{merge}	0.012
No. data ($F_{obs} > 3\sigma_F$)	654
R_u	0.033
R_w	0.032
Residual on difference maps (max e/Å^3):	
(+)	0.5
(−)	0.5

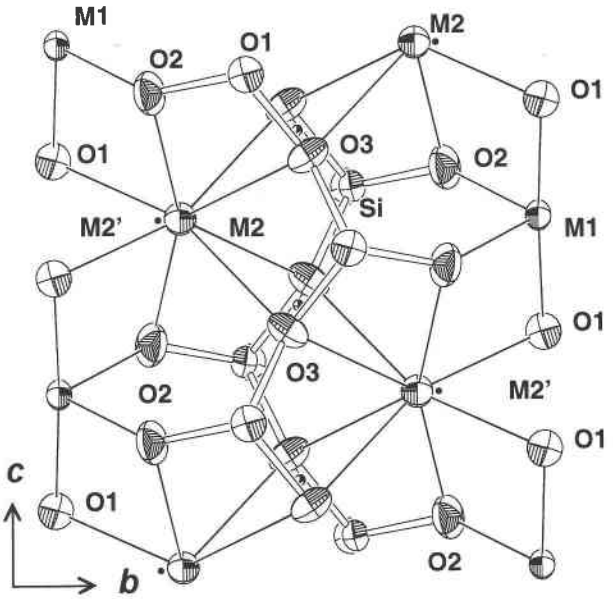

FIGURE 1. Projection of a slice of the structure of K18a clinopyroxene onto (100) showing the scaled vibrational ellipsoids except for M2′, which is represented as small solid circles. The small hatched circles between adjacent O3 ellipsoids are centers of symmetry.

FACS-I four-circle diffractometer. Details of the data collection and reduction are given in Table 1. Absorption corrections employed an empirical ψ-scan technique, utilizing intensity data obtained from ±180° ψ scans at 10° intervals for one reflection (060). Symmetry equivalent reflections were averaged (yielding R_{merge}), and only the reflections with $F_{obs} > 3\sigma_F$ were used in the structure determination and refinement.

Crystallographic calculations were made using the XTAL3.2 package, both UNIX and PC versions (Hall and Stewart 1992; Grossie 1992). Interpolated form factors of neutral atoms, including terms for anomalous dispersion (Davenport and Hall 1992), were used in all calculations, and all reflections were weighted as $1/\sigma$ in the least-squares refinements. Positional parameters of diopside from Cameron et al. (1973) were used to initiate the refinement, assigning Si to the T site; Fe, Al, and Cr to M1; Ca, K, and Na to M2; and Mg was split between M1 and M2 to balance site occupancy. A single scale factor and an extinction parameter were refined, and initial cycles of refinement used isotropic displacement parameters for each atomic site, *R* converging to 4.8%. In Fourier maps an excessively large anisotropy was obvious for the M2 site, aligned along *b*, so the splitting approach of Bruno et al. (1982) and Tribaudino et al. (1989) for Cpx on the diopside-enstatite (Di-En) join was adopted: M2 is split with the large ions averaged into the main centroid, and M2′, assigned all of the excess Mg, displaced ~0.33 Å toward M1 (see Fig. 1 and discussion below). Refinements proceeded with anisotropic displacement models except that M2′ was highly correlated with M2 and was therefore either treated as isotropic or constrained to have the same values of anisotropic displacement parameters as M2.

To assess the accuracy of the data and M site assignments several refinement strategies were used. With the assignments of the initial model above, the occupancy of a single high-*Z* species in each M site was permitted to vary independently to obtain a mean atomic number (m.a.n.) for the sites. These results are presented in Table 2 and compared with the initial assignments above made on the basis of the probe data and subsequent models. The refined sum of m.a.n. in M sites is slightly lower (0.5 e) than that derived from the microprobe composition. Considering that this ~1.5% difference is within other ranges of errors and that neutral rather than ionized atom-scattering factors were used, cation contents based on the probe-measured composition are reasonable. The largest difference in m.a.n. between the two refinements is in M1, so ordering of Mg and Fe among M1 and M2′ was examined; Table 3 gives the essential results. In model A, Mg-Fe exchange between M1 and M2′ was permitted by refining the occupancies (constrained to the measured composition) with M2 anisotropic and M2′ isotropic. Model B is the same, but the *U* values of M2 and M2′ were constrained to be equal. Finally, model C is the same as A, but the K content was refined independently

TABLE 2. Mean atomic number (m.a.n.) in M sites

	M1	M2	M2′	Σ M
Initial model	13.82	17.6	1.27	32.69
Refine m.a.n.	13.17(8)	17.54(48)	1.42(48)	32.14
Model A	13.24	17.6	1.85	32.69
Model B	13.37	17.6	1.72	32.69
Model C	13.18	17.37	1.91	32.46

TABLE 3. A comparison of different refinement models for K18a

	A	B	C
Site occups.	fix Ca,Na,K in M2 vary Mg and Fe: M1,M2′	same as A	same as A but unconstrained K
Thermal motion	M2 anisotropic M2′ isotropic	M2 = M2′ anisotropic	same as A
		M1	
y	0.9069(1)	0.9068(1)	0.9069(1)
B_{eq} (Å²)	0.57(3)	0.59(3)	0.54(3)
Occup.	0.885(3)[Mg] + 0.023[Fe]	0.877(3)[Mg] + 0.031[Fe]	0.889(4)[Mg] + 0.019[Fe]
(Fixed)	0.021[Al] + 0.071[Cr]	same	same
		M2	
y	0.3008(2)	0.3018(1)	0.3012(2)
B_{eq} (Å²)	0.77(2)	0.78(2)	0.74(2)
Occup.	0.073[K]	same	0.061(6)[K]
(Fixed)	0.798[Ca] + 0.023[Na]		0.798[Ca] + 0.023[Na]
		M2′	
y	0.264(3)	0.260(2)	0.264(3)
B (Å²)	3.9(8)	0.78	3.2(8)
Occup.	0.070[Mg] + 0.036(3)[Fe]	0.078[Mg] + 0.028(3)[Fe]	0.066[Mg] + 0.040(4)[Fe]
M2-M2′ (Å)	0.33(3)	0.37(2)	0.33(2)
R_u (%)	3.283	3.265	3.278
R_w	3.2	3.2	3.2

of composition to examine M2 content and its m.a.n. further. Differences among the models are small, so only the essential differences are given in Table 3, and the positional and displacement parameters (Table 4) and bond distances and selected angles (Table 5) for model A are given and used in comparisons with other structures. Table 6 lists the relative and calculated structure factors.[1]

[1] A copy of Table 6 may be ordered as Document AM-96-613 from the Business Office, Mineralogical Society of America, 1015 Eighteenth Street NW, Suite 601, Washington, DC 20036, U.S.A. Please remit $5.00 in advance for the microfiche.

DISCUSSION

The refinements of the K18a structure show K is indeed in the M2 site. Assignment of K to M2 is required to account for the electron density at that site and to yield a good refinement (low *R*). The refined, unconstrained K occupancy of M2, 0.061(6), is within two standard errors of the microprobe-derived value, 0.073(4), and the independently refined m.a.n. of M2 requires the 1.3 e contributed by K to attain the total of ~17.5. The average structure includes a subsidiary M2′ site displaced 0.33 Å from M2 along *b*. M2′ contains the residual Mg + Fe not in M1 and a higher proportion of Fe than M1: Mg/(Mg + Fe) = ~0.97 in M1 and ≤0.7 in M2′.

TABLE 4. Atom positions, occupancies, and displacement factors (Å²) and comparisons with other Cpx samples

	K18a diopside					Di_{100}		$Di_{90}En_{10}$	
Site	Occup.	*x*	*y*	*z*	*B*	Occup.	*B*	Occup.	*B*
M1	*	0	0.9069(1)	¼	0.57(3)	1 [Mg]	0.26(1)	0.99 [Mg]	0.38
M2	*	0	0.3008(2)	¼	0.77(2)	1 [Ca]	0.514(7)	0.87(1) [Ca] + 0.13 [Mg]	0.59
M2′	*	0	0.264(3)	¼	3.9(8)			0.04 [Mg]	0.59
T	0.996[Si] + 0.004[Al]	0.28726(8)	0.09254(9)	0.2300(2)	0.61(2)	1 [Si]	0.228(7)	1 [Si]	0.32
O1	1 [O]	0.1154(2)	0.0861(2)	0.1415(4)	0.85(5)	1 [O]	0.33(2)	1 [O]	0.42
O2	1 [O]	0.3621(2)	0.2498(2)	0.3193(4)	1.18(6)	1 [O]	0.46(2)	1 [O]	0.68
O3	1 [O]	0.3505(2)	0.0182(2)	0.9951(4)	0.89(5)	1 [O]	0.39(2)	1 [O]	0.52

Site	*U* (Å²)	U_{11}	U_{22}	U_{33}	U_{12}	U_{13}	U_{23}
M1	0.0072(4)**	0.0072(6)	0.0060(6)	0.0074(6)	0.0	0.0003(4)	0.0
M2	0.0097(3)**	0.0102(5)	0.0093(6)	0.0069(5)	0.0	−0.0020(3)	0.0
M2′	0.05(1)						
T	0.0077(2)**	0.0079(4)	0.0064(4)	0.0089(4)	−0.0003(3)	0.0023(3)	−0.0006(3)
O1	0.0108(6)**	0.0086(9)	0.012(1)	0.012(1)	0.0006(8)	0.0023(8)	−0.0000(8)
O2	0.0149(7)**	0.018(1)	0.009(1)	0.019(1)	−0.0044(8)	0.0073(9)	−0.0027(8)
O3	0.0113(6)**	0.0078(9)	0.015(1)	0.011(1)	−0.0002(8)	0.0025(8)	−0.0045(8)

* See Table 3.
** Equivalent isotropic value; $U = -8\pi^2\mu^2 = -8\pi^2 B$.

TABLE 5. A comparison of selected interatomic distances (Å) and angles (°)

Distance or angle	K18a diopside This study	Di_{100} Cameron et al. (1973)	$Di_{90}En_{10}$ Bruno et al. (1982)
M1-O1	2.126(1)	2.115(1)	2.125(2)
M1-O1	2.057(2)	2.065(2)	2.060(1)
M1-O2	2.047(2)	2.050(1)	2.056(2)
Mean (6)	2.077	2.077	2.080(2)
V (Å^3)	11.84	11.85	11.92
M2-O1	2.375(3)	2.360(1)	2.351(2)
M2-O2	2.338(2)	2.353(3)	2.314(2)
M2-O3	2.574(2)	2.561(2)	2.573(2)
M2-O3	2.729(2)	2.718(2)	2.729(2)
Mean (6)	2.429	2.425	2.413
Mean (8)	2.504	2.498	2.492
V (8) (Å^3)	25.89	25.76	25.53
M2′-O1	2.115(19)		1.843(1)
M2′-O2	2.297(2)		2.286(2)
M2′-O3	2.833(20)		3.127(1)
M2′-O3	2.938(16)		3.186(1)
Mean (4)	2.206		2.065
Mean (8)	2.546		2.429
M2-M2′	0.33(3)		0.69
Si-O1	1.610(2)	1.602(2)	1.601(1)
Si-O2	1.594(2)	1.585(1)	1.583(2)
Si-O3	1.665(2)	1.665(2)	1.665(2)
Si-O3	1.683(2)	1.687(2)	1.682(1)
Mean Si-O	1.638	1.635	1.633
σ	0.043	0.049	0.048
V	2.238	2.221	2.215
Ang. var.[2]	25.3	28.6	26.45
Si-O3-Si	136.4(1)	135.93(9)	136.2(1)
O3-O3-O3	165.9(1)	166.4(1)	165.6(1)
Tilting angle	2.75	2.53	2.76

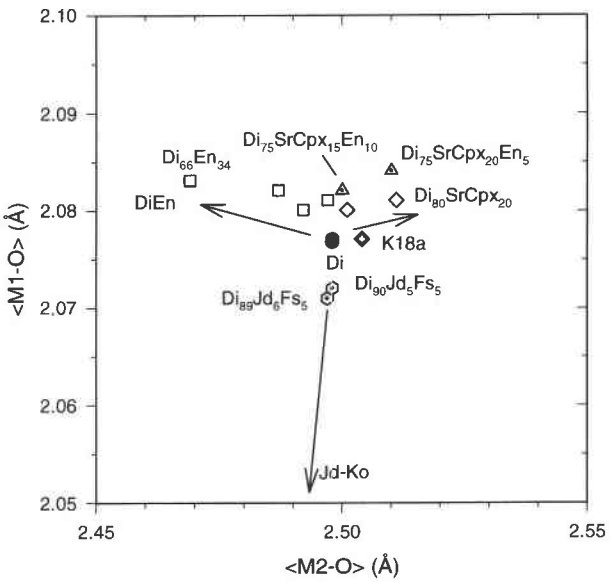

FIGURE 2. Plot of average M2-O (eight bonds) vs. average M1-O distances for K18a and other $C2/c$ diopsidic pyroxenes: solid diamond containing cross = K18a; solid circle = diopside (Di) of Cameron et al. (1973); squares = Di_{100}, $Di_{90}En_{10}$, $Di_{80}En_{10}$ of Bruno et al. (1982) and $Di_{66}En_{34}$ of Tribaudino et al. (1989); diamonds and triangles = $Di_{90}SrCpx_{10}$ and others as shown of Benna et al. (1987); hexagons = natural diopside samples of Rossi et al. (1983). Arrows indicate the Di-En, Di-SrCpx, and Di-Jd-Ko solid-solution trends.

Comparisons of K18a structural data with those showing the effect of various substitutions in M2, M2′, and M1 demonstrate the role of K in the complex solid solution. The average M2-O bond distance, ⟨M2-O⟩, in K18a is similar to that in diopside, but larger by 0.006 Å (Table 5). Data for $SrMgSi_2O_6$ (hereafter SrCpx) in solid solution with Di and En (Benna et al. 1987), Figure 2, show that the large Sr cation ($^{[8]}R$ = 1.26 Å) increases ⟨M2-O⟩ but also slightly increases ⟨M1-O⟩. Di-SrCpx-En Cpx has larger ⟨M1-O⟩, although the En content (which also expresses an M2′ site in these structures) decreases ⟨M2-O⟩, as it does in Di-En Cpx as shown. In addition to K and En content, K18a is affected by both jadeite (Jd) content and Cr (charge-balancing K), which both decrease ⟨M1-O⟩. Linear regressions of ⟨M-O⟩ and composition cannot be based on these data, which are insufficient for this purpose, but the net position of K18a in Figure 2, by balancing the above factors, manifests the expanding effect of K on ⟨M2-O⟩, the neutral to expanding effect of K on ⟨M1-O⟩, and the balancing effect of En with respect both to K on ⟨M2-O⟩ and Jd and Cr on ⟨M1-O⟩. Thus, K does have an expanding effect, but the small cations in M2 + M2′ largely counterbalance it to yield a diopside-like structure. This relationship can be further rationalized for these data by calculating the average M2 + M2′ cation radius as shown in Table 7. This calculation also indicates a large effective coordination number is required for Fe and Mg in M2′ to be consistent with the observed ⟨M2-O⟩. Another important feature visible in Figure 2 is that an increase of ⟨M1-O⟩ accompanies both an increase in ⟨M2-O⟩, as seen in the Di-SrCpx and noted in other Cpx by Cameron and Papike (1980), or dilution of M2 with En content. These effects would explain the apparently large ⟨M1-O⟩ value for K18a compared with a linear combination of the M1-site contents

TABLE 7. Rationalizing average M2 bond length and cation radius

	K18a diopside	Di_{100}	$Di_{90}En_{10}$
⟨M2-O⟩ (Å)	2.504	2.498	2.492
$R^{[4]}$O	−1.38	−1.38	−1.38
Effective R (Å)	1.124	1.118	1.112

Avg. M2 cation radius in K18a

$^{[8]}$M2: 0.798·1.12 Å^a + 0.073·1.51^b + 0.023·1.18^c = 1.031 Å

$^{[8]}$M2 + $^{[6]}$M2′: 0.798·1.12 Å^a + 0.073·1.51^b + 0.023·1.18^c + 0.036·0.78^d + 0.070·0.72^e = 1.110 Å

$^{[8]}$M2 + $^{[8]}$M2′: 0.798·1.12 Å^a + 0.073·1.51^b + 0.023·1.18^c + 0.036·0.92^f + 0.070·0.89^g = 1.127 Å

Occupancy averaged sum of ⟨$^{[6]}$M1-O⟩ vs. ⟨M1-O⟩ in K18a

0.885·2.077 Å^h + 0.023·2.130^i + 0.021·1.929^j + 0.071·2.010^k = 2.070 vs. 2.077 Å^l

Note: a = $R^{[6]}$Ca, b = $^{[6]}$K, c = $^{[8]}$Na, d = $^{[6]}$Fe, e = $^{[6]}$Mg < $R^{[6]}$Obs, f = $^{[8]}$Fe, g = $^{[6]}$Mg ≈ $R^{[8]}$Obs, h = ⟨Mg-O⟩, i = ⟨Fe-O⟩, j = ⟨Al-O⟩, k = ⟨Cr-O⟩, and l = ⟨M1-O⟩.

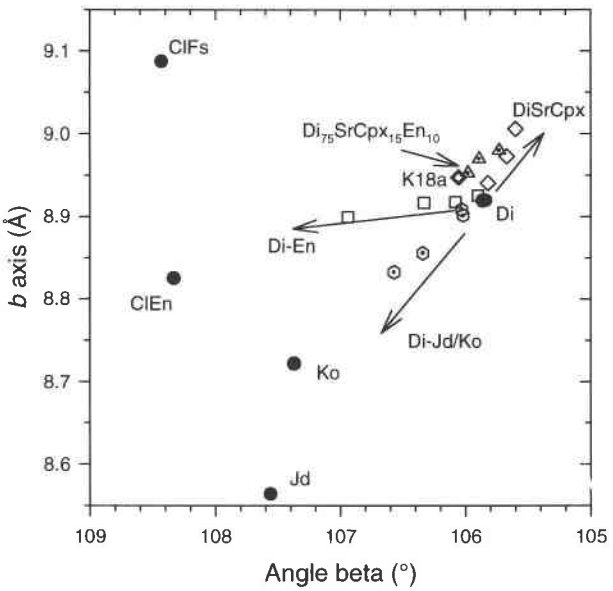

FIGURE 3. Plot of cell parameters β vs. b with the same symbols as in Figure 2 except that Di is from Clark et al. (1969), jadeite (Jd) and kosmochlor (Ko) are from Cameron et al. (1973), clinoenstatite (ClEn) is from Morimoto et al. (1960), and clinoferrosilite (ClFs) is from Burnham (1967).

multiplied by the average ⟨M1-O⟩ for the end-members (the approach of Rossi et al. 1983) in Table 7.

Some effect on Si-O distances might be expected from the changes in M-site occupancies. The ⟨Si-O⟩ in K18a is slightly longer than in diopside, which may be a result of the 0.4% $^{[4]}$Al content attributed by microprobe analysis. However, equivalent ⟨Si-O⟩ values are found in some Di-En-SrCpx (Benna et al. 1987), so the small change may also be due to the slight enlargement of M2 caused by K content. Lengthening of Si-O1 and Si-O2 distances relative to diopside is likely attributable to the trivalent cations in M1, but decreases in the two Si-O3 distances, yielding smaller ⟨Si-O⟩ as in Cpx along the Di-Jd join (e.g., Oberti and Caporuscio 1991), are not found in K18a.

The modifications to the structure by the presence of K in a complex solid solution are also manifest in the lattice dimensions, as first noted for V by Harlow and Veblen (1991). The b vs. β plot in Figure 3, as in Benna et al. (1987), presents the Di-Jd-En-SrCpx data along with various Cpx end-members (clinoenstatite and clinoferrosilite have $P2_1/c$ structures; the others have $C2/c$ structures). The arrows indicate the trends for Di-SrCpx, Di-En, and Di-Jd-Ko (Ko = kosmochlor) solid solutions, and the position of K18a near $Di_{75}SrCpx_{15}En_{10}$ indicates the competing effect of K to decrease β and increase b (like Sr) with the effects of En-Fs content to increase β and Jd-Ko (and Cr-balancing K) content to increase β and decrease b. An important aspect is that significant K content of a Cpx should be manifest in the lattice parameters once competing compositional effects have been considered.

A conspicuous difference in the structures presented in Table 5 is seen the values for apparent atomic thermal motion, B or U, which are a measure of positional averaging whether from thermal motion or average structure. Some of the variance could be due to differences among the refinement models, as discussed by Armbruster et al. (1990) in their study of low albite refinements. However, the data collection and refinement strategies among the compared structures are very similar [e.g., similar maximum (sin θ)/λ, neutral atoms for K18a and several others, no assigned vacancies, etc.], and there is essentially no Al-Si contribution to disorder, so the differences are not simply an artifact. Diopside has the smallest equivalent isotropic B values, which is consistent with it being fully ordered and not an average structure. The B values for $Di_{90}En_{10}$ are 20–50% larger and those for K18a are ~2–3 times larger. Even the $Di_{66}En_{34}$ Cpx studied by Tribaudino et al. (1989) has only moderately greater values of B for a Cpx with a much more disordered M2 site. Likewise, the root-mean-squared displacements for "thermal" ellipsoids are larger for K18a than Di_{100} or $Di_{90}En_{10}$ by factors from 1.02 to 1.80, but there are no conspicuous changes in the anisotropies (e.g., ratios of maximum to minimum displacements) (Table 8). However, in the $Di_{66}En_{34}$ structure (Tribaudino et al. 1989), which was modeled with split O atoms to accommodate separate M2-O and M2′-O coordination polyhedra, the site anisotropies are generally one-half larger than in K18a. The generalizations are that the O displacements are increased the most, and M2 is the least enlarged ellipsoid with no increased anisotropy. The mixed-size contents of the cation sites manifest their individual effects in larger ellipsoid displacements, particularly for the bonded O atoms, but there is no systematic change in positional averaging vs. thermal motion, at least to the extent that 7% K (and 2% Na) is averaged into M2 in the K18a Cpx.

The orientations of the vibrational ellipsoids for M and O sites do not vary greatly among the compared diopsidic Cpx structures (e.g., Table 8), suggesting that the basic nature of the structure is to accommodate distortion from thermal or averaged displacements in a consistent manner. Vibrational ellipsoids for O2 and O3 are the largest and most anisotropic, and the maximum displacement (axis 3) vectors are generally aligned along the M2-O bond direction, [M2-O]. Angles [M2-O] $\wedge$ [O-axis 3] are 19° for O2 and 32 and 35° for the two O3 in K18a, and 83° for O2 and 32 and 35° in Di_{100}; O2 shows the displacive effect of M2 disorder. These same displacements are generally perpendicular to the respective Si-O bonds: Angles [T-O] $\wedge$ [O-axis 3] are 86° for O1, 97° for O2, and 97 and 94° for O3 in K18a (see Fig. 1), and 85° for O1, 84° for O2, and 96 and 95° for O3 in Di_{100}. These features indicate that local thermal or displacive changes in M-O bonds are accommodated by either tetrahedral bond bending or whole tetrahedral rotation or libration around an Si-O1 axis. The bond-bending possibility is not the source of the anisotropy because the projection of the Si

TABLE 8. Ellipsoids of apparent thermal motion

	K18a diopside This study				Di_{100} Cameron et al. (1973)				$Di_{90}En_{10}$ Bruno et al. (1982)			
		angle with				angle with				angle with		
Axis	RMS Ampl (Å)	*a*	*b*	*c*	RMS Ampl (Å)	*a*	*b*	*c*	RMS Ampl (Å)	*a*	*b*	*c*
						M1						
1	0.077(3)	52(10)	90	55(10)	0.052(3)	56(10)	90	49(10)	0.057(4)	102(6)	90	152(6)
2	0.077(3)	90	180	90	0.055(3)	90	180	90	0.072(3)	90	0	90
3	0.098(5)	142(10)	90	35(10)	0.065(2)	146(10)	90	41(10)	0.077(3)	168(6)	90	62(6)
						M2						
1	0.070(3)	62(3)	90	43(3)	0.066(1)	66(1)	90	39(1)	0.057(2)	116(2)	90	143(2)
2	0.096(3)	90	180	90	0.068(1)	90	180	90	0.094(2)	90	0	90
3	0.122(3)	153(3)	90	47(3)	0.103(1)	156(1)	90	50(1)	0.101(2)	160(2)	90	53(2)
						T						
1	0.079(3)	86(10)	13(6)	79(7)	0.049(2)	27(17)	72(20)	85(9)	0.056(2)	168(11)	102(9)	78(9)
2	0.089(3)	173(14)	85(11)	79(15)	0.053(2)	67(20)	155(17)	106(11)	0.062(2)	101(12)	48(8)	41(8)
3	0.095(2)	96(15)	102(6)	16(12)	0.059(1)	105(8)	107(11)	17(11)	0.071(2)	84(5)	136(7)	51(7)
						O1						
1	0.092(5)	20(13)	101(14)	89(13)	0.051(4)	30(9)	98(9)	77(8)	0.061(4)	155(10)	78(10)	95(11)
2	0.107(5)	95(21)	160(54)	107(61)	0.069(3)	65(14)	45(35)	132(34)	0.076(3)	106(23)	71(64)	18(62)
3	0.111(5)	109(13)	107(60)	17(61)	0.073(3)	105(17)	46(35)	44(34)	0.079(4)	107(21)	157(54)	72(65)
						O2						
1	0.085(6)	69(6)	23(4)	87(6)	0.050(4)	62(3)	30(3)	87(5)	0.065(4)	118(4)	146(3)	98(5)
2	0.124(6)	41(8)	101(7)	145(8)	0.079(3)	103(7)	72(6)	146(8)	0.095(3)	49(7)	97(6)	153(7)
3	0.147(4)	56(7)	110(3)	55(8)	0.094(3)	149(5)	67(4)	56(8)	0.112(3)	125(7)	57(3)	111(7)
						O3						
1	0.087(7)	12(66)	101(43)	110(65)	0.058(4)	113(27)	59(6)	33(8)	0.063(4)	80(15)	108(4)	161(5)
2	0.091(6)	100(79)	121(19)	139(42)	0.064(3)	156(26)	96(15)	98(23)	0.075(4)	13(12)	94(7)	94(14)
3	0.134(4)	97(5)	146(5)	56(5)	0.085(3)	97(6)	148(5)	59(5)	0.101(3)	98(5)	161(4)	71(4)

Note: Angles in degrees.

and O thermal displacements along the separation vector are so similar, a characteristic that has been interpreted as an indicator that silica tetrahedra are rigid bodies (Downs et al. 1990, 1992). Consequently, an element of flexibility in the structure appears to be local chain bending at O3 for both thermal motion and M disorder.

Resolution of the explicit effects of K in M2 of Cpx probably requires either a larger K content than examined here or a different analytical technique. Experimental samples with ~0.15 K per formula unit and simpler Ca-Na-K-Cr-Mg and Ca-Na-K-Al-Mg Cpx composition [Harlow (1994) and in preparation] are now being prepared for structure refinement to resolve the issue.

CONCLUSION

This refinement is yet more evidence confirming the existence of K in Cpx at high pressure. Given the critical role of Al or Cr in M1 of a diopsidic pyroxene in permitting K incorporation by means of charge-balanced exchange, the pressure dependence of jadeite component stability and both jadeite and kosmochlor miscibility in diopside (Ikeda and Yagi 1972; Vredevoogd and Forbes 1975) must be considered as well as the bulk composition of a Cpx-bearing rock. These factors work with the relatively high polyhedral compressibility of K compared with Ca (derived from the bulk moduli of alkali and alkaline earth salts; see Hazen and Finger 1982, Hazen 1988) for compatibility of K in diopsidic Cpx at high pressure.

Another factor to be addressed from the results presented here is the role of Mg in M2′ as a stabilizer of K in Cpx. At formational conditions there is undoubtedly a single M2 site (Tribaudino et al. 1989) in which Ca and Mg are mixed, and, from the coexisting En lamellae, it must be assumed that the original En content of the K18a Cpx was higher, perhaps En_{30}. Going from 5 to 10 GPa, the position of the En-poor part of the Di-En solvus rises by about 100 °C (Gasparik 1990), so En-Di solubility does not by itself facilitate K uptake if temperature has an inverse effect compared with pressure, as it usually does. Clearly Mg in M2 balances the large size of K in M2 in the ambient structure, so En-Di solubility must be added to the factors that permit K uptake in mantle Cpx and establish the P-T-a_K conditions at which the K18a inclusion was formed. The temperature should be a minimum of 1450–1550 °C, estimating a formational content of En_{30} (Gasparik 1990), the high end of the T estimates (Harlow and Veblen 1991). Thus, with present estimates of the distribution coefficient at P and 1500 °C [$D_K^{Cpx/L}$ = 0.03–0.06 from Harlow (1994) and in preparation] and a lowered K_2O content of 1.2 wt%, the pressure and the crystallizing fluid-melt composition must have been high, e.g., 40 wt% K_2O at 5 GPa or 20 wt% at 10 GPa.

ACKNOWLEDGMENTS

I thank Adrian Brearley, Bob Downs, and an anonymous reviewer for their very helpful comments and Eric Dowty for discussion. The K18a

crystal was loaned by John Gurney, University of Capetown. Financial support provided by the National Science Foundation (EAR-8916687 and EAR-9314819) is gratefully acknowledged.

References cited

Armbruster, T., Bürgi, H.B., Kunz, M., Gnos, E., Brönnimann, S., and Lienert, C. (1990) Variation of displacement parameters in structure refinements of low albite. American Mineralogist, 75, 135–140.

Benna, P., Chiari, G., and Bruno, E. (1987) Structural modifications in clinopyroxene solid solutions: The Ca-Mg and Ca-Sr substitutions in the diopside structure. Mineralogy and Petrology, 36, 71–84.

Bruno, E., Carbonin, S., and Molin, G. (1982) Crystal structures of Ca-rich clinopyroxenes on the $CaMgSi_2O_6$-$Mg_2Si_2O_6$ join. Tschermaks Mineralogische-Petrographische Mitteilungen, 29, 223–240.

Burnham, C.W. (1967) Ferrosilite. Carnegie Institution of Washington Year Book, 65, 285–290.

Cameron, M., Sueno, S., Prewitt, C.T., and Papike, J.J. (1973) High-temperature crystal chemistry of acmite, diopside, hedenbergite, jadeite, spodumene, and ureyite. American Mineralogist, 58, 594–618.

Cameron, M., and Papike, J.J. (1980) Crystal chemistry of silicate pyroxenes. In Mineralogical Society of America Reviews in Mineralogy, 7, 5–92.

Clark, J.R., Appleman, D.E., and Papike, J.J. (1969) Crystal-chemical characterization of clinopyroxenes based on eight new structure refinements. Mineralogical Society of America Special Paper, 2, 31–50.

Davenport, G., and Hall, S.R. (1992) ADDREF. In S.R. Hall and J.M. Stewart, Eds., XTAL 3.2 reference manual, p. 53–59. University of Western Australia, Perth.

Downs, R.T., Gibbs, G.V., and Boisen, M.B., Jr. (1990) A study of the mean-square displacement amplitudes of Si, Al, and O atoms in framework structures: Evidence for rigid bonds, order, twinning, and stacking faults. American Mineralogist, 75, 1253–1267.

Downs, R.T., Gibbs, G.V., Bartelmehs, K.L., and Boisen, M.B., Jr. (1992) Variations of bond lengths and volumes of silicate tetrahedra with temperature. American Mineralogist, 77, 751–757.

Gasparik, T. (1990) A thermodynamic model for the enstatite-diopside join. American Mineralogist, 75, 1080–1091.

Grossie, D.A. (1992) XTAL 3.2 for IBM compatible 386-based PCs. Department of Chemistry, Wright State University, Dayton, Ohio.

Hall, S.R., and Stewart, J.M. (1992) XTAL 3.2 Reference Manual. University of Western Australia, Perth.

Harlow, G.E. (1994) High-*P* partitioning of K between Cpx and K-carbonate. Eos, 75, 369.

Harlow, G.E., and Veblen, D.R. (1991) Potassium in clinopyroxene inclusions from diamonds. Science, 251, 652–655.

Hazen, R.M. (1988) A useful fiction: Polyhedral modeling of mineral properties. American Journal of Science, 288-A, 242–269.

Hazen, R.M., and Finger, L.W. (1982) Comparative crystal chemistry. In Structural variations with pressure (chapter 7), p. 147–164. Wiley, New York.

Ikeda, K., and Yagi, K. (1972) Synthesis of Kosmochlor and phase equilibria in the join $CaMgSi_2O_6$-$NaCrSi_2O_6$. Contributions to Mineralogy and Petrology, 36, 63–72.

McCandless, T.E., and Gurney, J.J. (1986) Sodium in garnet and potassium in clinopyroxene: Criteria for classifying mantle eclogites. In Geological Society of Australia Special Publication 14, p. 827–832. Blackwell Scientific, Victoria.

Morimoto, N., Appleman, D.E., and Evans, H.T., Jr. (1960) The crystal structures of clinoenstatite and pigeonite. Zeitschrift für Kristallographie, 114, 120–147.

Oberti, R., and Caporuscio, F.A. (1991) Crystal chemistry of clinopyroxenes from mantle eclogites: A study of the key role of the M2 site population by means of crystal-structure refinement. American Mineralogist, 76, 1141–1152.

Prinz, M., Manson, D.V., Hlava, P.F., and Keil, K. (1975) Inclusions in diamonds: Garnet lherzolite and eclogite assemblages. In Physics and Chemistry of the Earth, 9, 797-815.

Rickard, R.S., Harris, J.W., Gurney, J.J., and Cardoso, P. (1989) Mineral inclusions in diamonds from the Koffiefontein Mine. In Geological Society of Australia Special Publication, 14, 1054–1062.

Rossi, G., Smith, D.C., Ungaretti, L., and Domeneghetti, M.C. (1983) Crystal-chemistry and cation ordering in the system diopside-jadeite: A detailed study by crystal structure refinement. Contributions to Mineralogy and Petrology, 83, 247–258.

Shannon, R.D. (1976) Revised effective ionic radii and systematic studies of interatomic distances in halides and chalcogenides. Acta Crystallographica, A32, 751–757.

Sobolev, N.V., Barkamenko, I.T., Yefimova, E.S., and Pokhilenko, N.P. (1991) Morphological features of microdiamonds, sodium in garnets and potassium in pyroxene from two eclogite xenoliths from Udachnaye kimberlite pipe, Yakutia. Doklady Akademia Nauk SSSR, 321, 585–592.

Tribaudino, M., Benna, P., and Bruno, E. (1989) Average structure and M2 site configurations in *C2/c* clinopyroxenes along the Di-En join. Contributions to Mineralogy and Petrology, 103, 452–456.

Vredevoogd, J.J., and Forbes, W.C. (1975) The system diopside-ureyite at 20 kb. Contributions to Mineralogy and Petrology, 52, 147–156.

Manuscript received June 13, 1995
Manuscript accepted January 2, 1996